frontiers in Chemistry

ORIGINAL RESEARCH
published: 22 March 2022
doi: 10.3389/fchem.2022.856832

The Synthesis of Picolinamide-Supported Tetracoordinated Organoboron Complexes with Aggregation-Induced Emission Property

Gaoqiang You, Liang Xu and Yu Wei**

Key Laboratory for Green Processing of Chemical Engineering of Xin-Jiang Bingtuan, School of Chemistry and Chemical Engineering, Shihezi University, Shihezi, China

The picolinamide-supported tetracoordinated organoboron complexes containing diaryl boronyl segments have been synthesized for the first time. Aryl trifluoroborates were utilized as the BAr_2 sources to introduce different aryl motifs with diverse functional groups. The optical experiments discovered these five-membered boron-containing complexes were aggregation-induced emission (AIE) active, thus affording a new class of AIE molecules.

Keywords: tetracoordinated organoboron, AIE, picolinamide, potassium trifluoroborate, manganese

OPEN ACCESS

Edited by:
Jamal Rafique,
Federal University of Mato Grosso do Sul, Brazil

Reviewed by:
Zhao Chen,
Jiangxi Science and Technology Normal University, China
Dario Pasini,
University of Pavia, Italy

****Correspondence:***
Liang Xu
xuliang4423@shzu.edu.cn
Yu Wei
yuweichem@shzu.edu.cn

Specialty section:
This article was submitted to Organic Chemistry, a section of the journal Frontiers in Chemistry

Received: *17 January 2022*
Accepted: *21 February 2022*
Published: *22 March 2022*

Citation:
You G, Xu L and Wei Y (2022) The Synthesis of Picolinamide-Supported Tetracoordinated Organoboron Complexes with Aggregation-Induced Emission Property. Front. Chem. 10:856832. doi: 10.3389/fchem.2022.856832

INTRODUCTION

Taking advantage of the vacant *p*-orbitals of the boron atoms, the chelating complexation between π-conjugated ligands and -BR_2 units will generate tetracoordinated organoboron complexes containing X→B dative bonds that are able to lock the π-conjugated ligands. These modifications will enhance the molecular rigidity, extend the π-conjugation system, and thus afford molecules with superior photoluminescence properties (Chen et al., 2017; Dou et al., 2017; Mellerup and Wang, 2019; Yan et al., 2019; Huang et al., 2020). Therefore, over the past decades, the synthesis, improvement, and application of these tetracoordinated organoboron complexes have attracted a continuing interest from organic and materials communities. However, the emission of these planar structures in aggregates or the solid-state is usually spoiled due to the aggregation-caused quenching (ACQ) effects. This limits their applications in organic optoelectronic materials or other situations that demand solid-state emissions, such as organic lasers and organic light-emitting diodes (OLEDs), which necessitates the development of new series of these complexes with high solid-state luminescence efficiency.

Since the conceptualization of the aggregation-induced emission (AIE) effect by the Tang group in 2001 (Luo et al., 2001; Mei et al., 2015), many types of AIE-active compounds/units have been developed. In recent years, a number of AIE-active tetracoordinated organoboron complexes have been synthesized and applied as aggregate-state emitters (Virgili et al., 2013; Liu et al., 2019; Nitti et al., 2020; Ito et al., 2021; Yin et al., 2021; Min et al., 2022). These AIE-active complexes, which are usually obtained *via* linking AIE-active units such as tetraphenylethylene (TPE) or introducing rotational aryls onto the chelating backbones, mostly contain BF_2 segments. The introduction of BAr_2 segments, which had two bulky aryl rings on boron atoms, has been utilized to disrupt the intermolecular π–π stacking in aggregate states and thus enable more efficient AIE effects (**Figure 1**). Based on our survey, most of the known AIE-active complexes with BAr_2 segments were six-

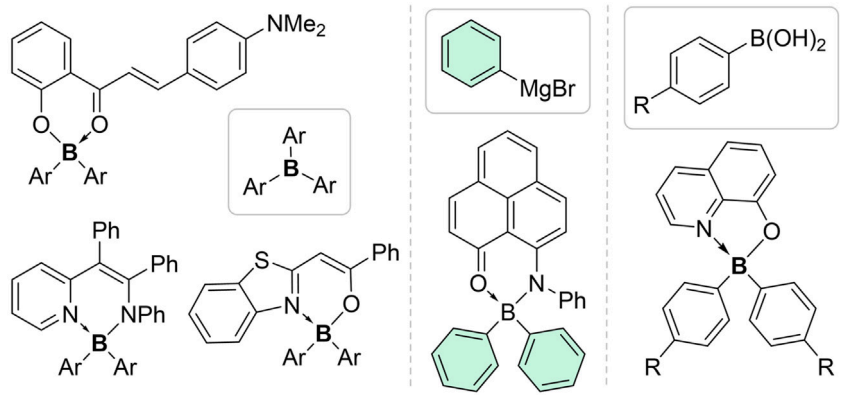

FIGURE 1 | The tetracoordinated organoboron complexes containing BAr_2 segments with AIE properties. The aryl precursors are indicated in the boxes.

TABLE 1 | Optimization of reaction conditions[a].

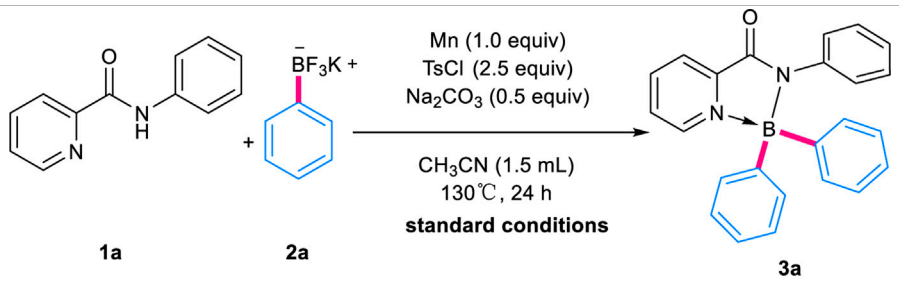

Entry	Variations from the standard conditions	Yields (%)[b]
1	None	99
2	Without Mn	81
3	Without TsCl	N.R.
4	Without Na_2CO_3	24
5	DMF instead of MeCN	Trace
6	DMA instead of MeCN	Trace
7	THF instead of MeCN	Trace
8	NMP instead of MeCN	Trace
9	DMSO instead of MeCN	Trace
10	HFIP instead of MeCN	Trace
11	90°C instead of 130°C	N.R.
12	110°C instead of 130°C	66
13	K_3PO_4 instead of Na_2CO_3	24
14	Cs_2CO_3 instead of Na_2CO_3	27
15	LiOH instead of Na_2CO_3	41
16	$PhBF_3K$ (4.0 equiv)	41
17	$PhBF_3K$ (3.0 equiv)	23

[a]*Reaction conditions:* ***1a*** *(0.15 mmol),* ***2a*** *(0.75 mmol, 5 equiv), air, CH_3CN (1.5 ml), 130°C, 24 h.*
[b]*Isolated yields.*

membered. To the best of our knowledge, the only AIE-active five-membered cases have been disclosed very recently by Yang and Zou group (Qi et al., 2021). This was surprising since five-membered tetracoordinated organoboron compounds were very commonly encountered in organoboron-based molecules and materials. Moreover, BAr_2 segments were usually introduced via Ar_3B or aryl organometallic reagents (Kubota et al., 2012; Yan et al., 2014; Gong et al., 2015; Wang et al., 2015; Wu et al., 2015), limiting the accessibility and diversity of the target molecules (Yang et al., 2021).

On the other hand, innumerable chelating backbones have been applied in the complexation formation of tetracoordinated organoboron, to fine-tune the desirable luminescence properties. In this regard, it is surprising that picolinamide, one of the most available and widely-used chelating ligands in coordination chemistry, has never been used in the preparation of

TABLE 2 | Optimization of reaction conditions[a].

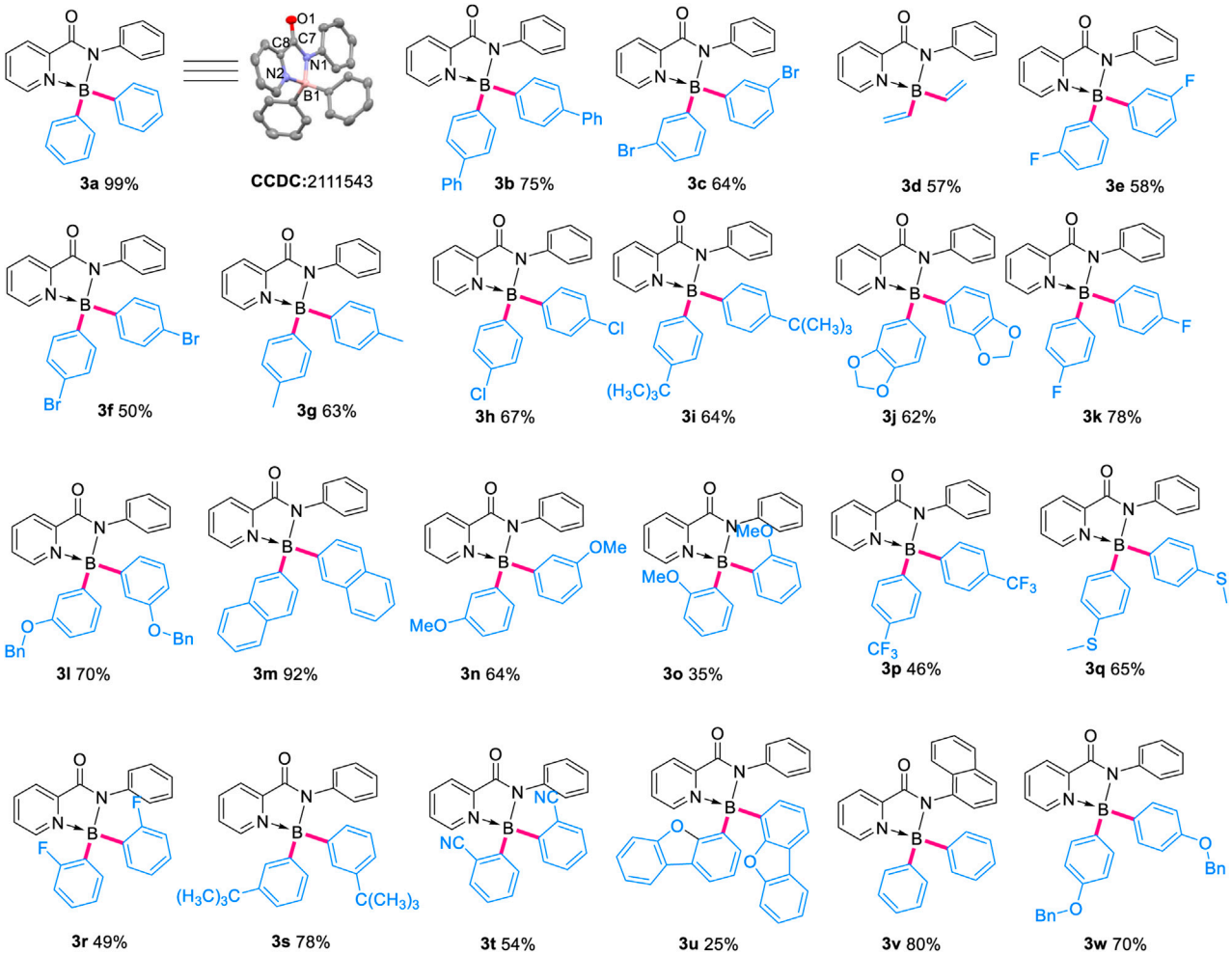

[a]*Reaction conditions: pyridinecarboxamide* ***1*** *(0.15 mmol), potassium aryl trifluoroborate* ***2*** *(0.75 mmol, 5 equiv), air, CH_3CN (1.5 ml), 130°C, 24 h.*

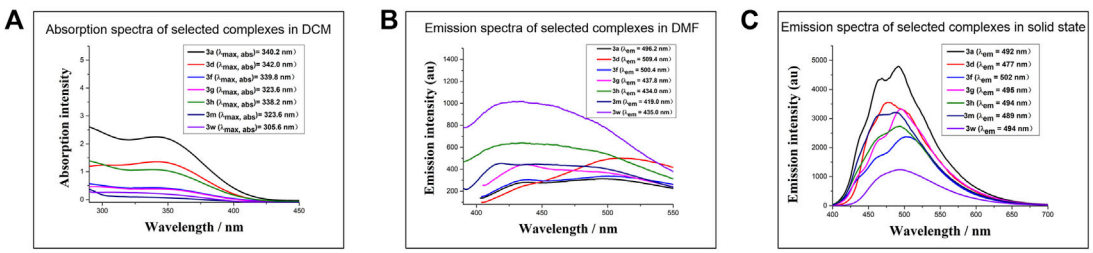

FIGURE 2 | The absorption and emission spectra of selected complexes.

tetracoordinated organoboron, to the best of our knowledge (Yang et al., 2021). Thus, we hypothesized that complexation between picolinamide and BAr_2 segments would afford a new series of tetracoordinated organoboron molecules. These complexes should adopt propeller structures and be consisted of electron-deficient pyridyl, electron-rich anilino groups, and the spiro linker centers of boron atoms, which potentially circumvent the trade-off between the complexation stability and the solid-

TABLE 3 | Luminescence quantum yield and lifetime of selected complexes.

	3a	3d	3f	3g	3h	3m	3w
Φ_{liquid} (%)[a]	0.31	0.39	0.39	0.64	0.59	1.02	1.09
τ_{liquid} (ns)[a]	1.99	1.86	1.91	1.76	2.03	1.86	2.01
Φ_{solid} (%)	78.38	82.46	44.26	89.54	97.83	82.96	31.48
τ_{solid} (ns)	3.64	4.29	3.01	3.84	3.31	2.98	3.29

[a]*Sample concentration 10^{-4} M.*

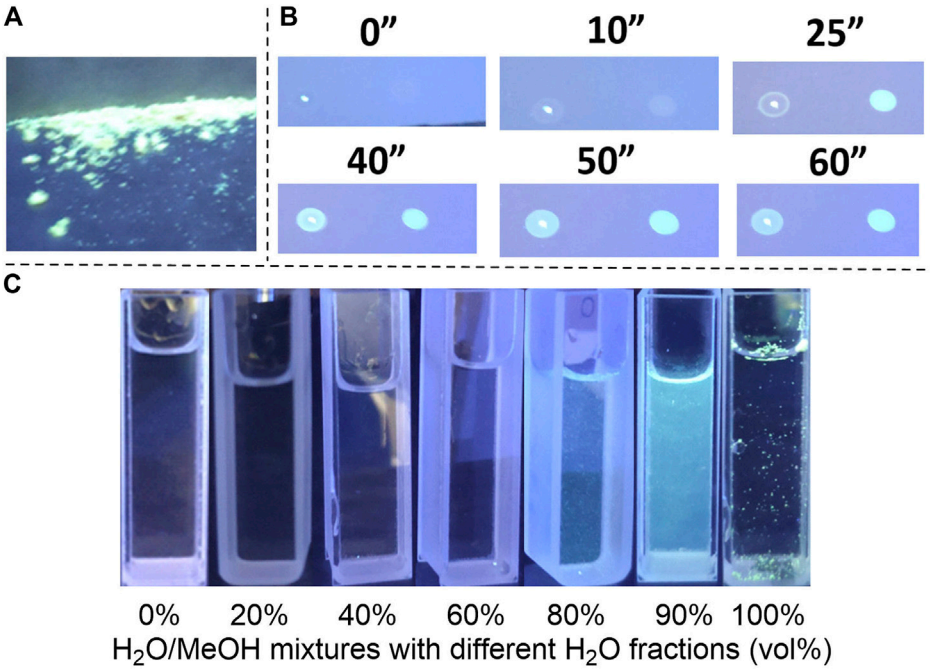

FIGURE 3 | AIE behaviours of **3a**. **(A) 3a** solid at 365 nm. **(B)** Fluorescence comparison of **3a** solution at 365 nm at different time. **(C)** Fluorescence comparison of **3a** at 365 nm in different ratios of water/methanol.

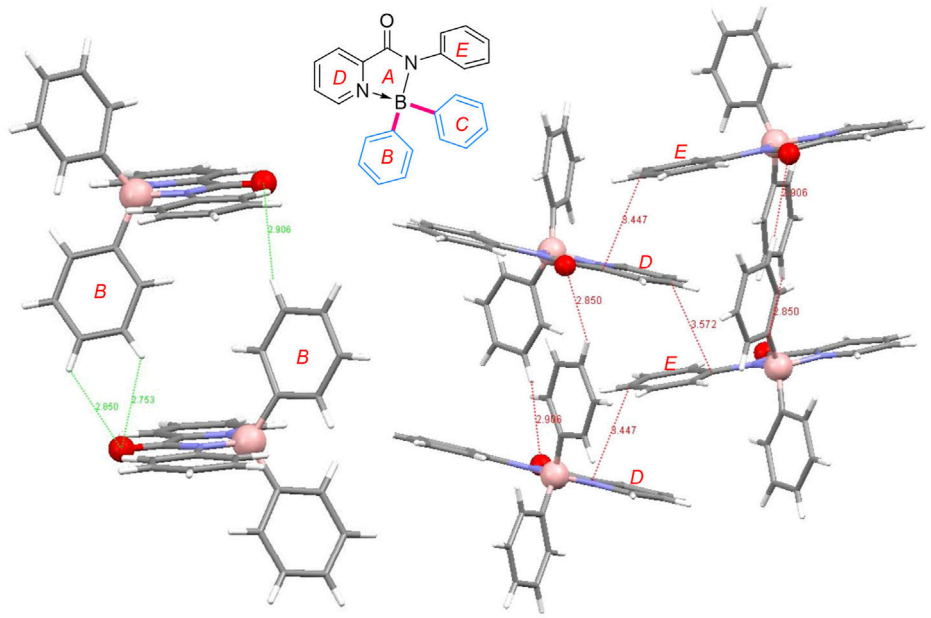

FIGURE 4 | The crystal structure of **3a**.

state luminescence, leading to some special light-emitting molecules (Shiu et al., 2016). The proposal would pose at least two major challenges: 1) to properly introduce the relatively flexible picolinamide ligands and 2) to bypass the traditional organometallic BAr_2 incorporation pathways.

RESULTS AND DISCUSSION

With these considerations in mind, the investigation was initiated by exploring the reaction between *N*-phenylpyridinecarboxamide **1a** and potassium phenyltrifluoroborate **2a** (Sawazaki et al., 2018; Wang

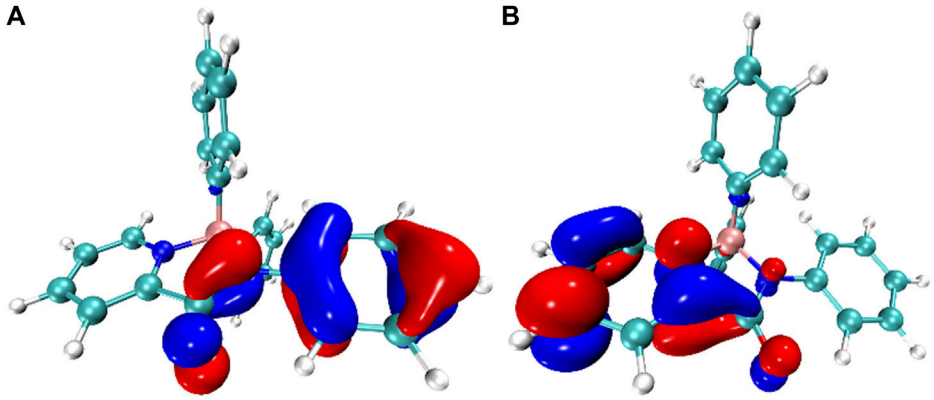

FIGURE 5 | The calculated HOMO **(A)** and LUMO **(B)** orbitals of **3a**.

et al., 2019), which has been demonstrated to be a competent BPh_2 provider recently by Song group (Yang et al., 2018) and our group (Zu et al., 2020) (**Table 1**). After systematic evaluation of reaction variables, to our delight, under similar reaction conditions with our previous work (Zu et al., 2020), the target product **3a** could be isolated in 99% yield by using Mn (1.0 equiv), *p*-toluenesulfonyl chloride (TsCl, 2.5 equiv) and Na_2CO_3 (0.5 equiv) in acetonitrile (CH_3CN) at 130°C for 24 h (entry 1). The propeller structure of **3a** was confirmed unambiguously *via* X-ray diffraction analysis of its crystals (**Table 2**).

Subsequently, control experiments were performed to elucidate the function of Mn, TsCl and Na_2CO_3 in these conditions (entry 2–4). It was found TsCl played a vital role in the formation of **3a**, in view that its absence would suppress the reaction totally. Omitting Mn from the conditions, still, 81% isolated yield of **3a** could be obtained, while the omission of Na_2CO_3 led to the formation of **3a** in only 24% yield. Further evaluation revealed the choice of solvent was also critical (entry 5–10). Other commonly-used organic solvents, including DMF, THF and DMSO, afforded only a trace amount of product **3a**. Moreover, the test of the reaction temperature showed the yield dropped sharply while lowering the temperature (entries 11–12). The investigation of a variety of bases showed that Na_2CO_3 performed best (entries 13–15). The reduction of the amount of **2a** also affected the yields remarkably (entries 16–17).

With the optimal conditions in hand, the substrate scope of this methodology was then investigated (**Table 2**). A broad scope of aryl trifluoroborates containing *para- ortho-* and *meta-*substituents were applied in the reactions successfully. Generally, the *ortho*-substituted aryl trifluoroborates gave lower isolated yields, in comparison with their *para-* and *meta*-substituted analogs, mainly due to the steric effect (**3e**, 58% vs. **3k**, 78% vs. **3r**, 49%; **3n**, 64% vs. **3o**, 35%). The reaction tolerated bromides and chlorides well (**3c**, **3f, 3h**), allowing the formation of halogenated products and thus leaving ample space for further decorations. No matter electron-withdrawing (-CF_3, -halides, -CN) or -donating (-OMe, -^{t}Bu, -OBn) groups were on the aryl trifluoroborates, the target boronyl complexes could be obtained in moderate to good yields. While aryl substrates containing π-extended systems were applied, products with more congested BAr_2 segments, like **3b**, **3m** and **3u**, were obtained. Notably, potassium vinyl fluoroborate proceeded smoothly to provide **3d** in moderate yields. When the *N*-substituent of pyridinecarboxamide was changed to 1-naphthyl, 80% of **3v** could be isolated.

Then, photophysical properties of the obtained complexes in solvent and in the solid-state were measured. As shown in **Figure 2** and **Table 3**, the selected complexes possessed very weak luminescence in organic solvent DMF along with very low quantum yield ($\Phi_{liquid} < 0.015$), probably due to the non-radiative process in the solvent induced by intramolecular rotation. In contrast, the solid-state spectra of the BAr_2-species showed intense emission bands centered around 490 nm with high quantum yield (Φ_{solid}: 31–98%), indicating the existence of AIE phenomenon and the absence of strong intermolecular π-π interactions in the solid-state.

Furthermore, the emission properties of **3a** were investigated in detail to prove its AIE behaviors (**Figure 3**). Firstly, under irradiation with a UV lamp at 365 nm, solid **3a** showed macroscopical fluorescence (**Figure 3A**). Then, **3a** was dissolved in H_2O/MeOH mixtures with different H_2O content (**Figure 3C**). When the H_2O content is lower than 60%, **3a** was dissolved totally and the solution was transparent without observable fluorescence. As the water content increased from 80 to 90%, **3a** became insoluble in the solvents and began to aggregate. Correspondingly, the turbidity and luminescence (at 365 nm) of the solution increased, which could be observed with the naked eyes. **3a** would disperse in the pure water with its aggregation showing the same luminescence as the solid-state. The AIE behavior of **3a** was further verified by observing the fluorescent changes during the evaporation of MeOH and THF solution of **3a** (**Figure 3B**). On a thin-layer chromatography plate, as the solvent evaporated and **3a** molecules aggregated, a clear increase in the fluorescence was observed under UV irradiation at 365 nm.

In order to better understand the AIE properties of these complexes, X–ray crystallographic analysis of **3a** was performed. As shown in **Figure 4**, the boron atoms of **3a** adopted a typical

tetrahedral geometry to form *N,N*–chelated five-membered rings. The pyridyl N→B bond lengths are around 0.03 Å longer than the amide N–B bonds. As anticipated, **3a** adopt twisted conformations and the two phenyl rings on the boron atom were not coplanar. The dihedral angles of A and B, A and C, B and C were 76.50°, 78.02° and 61.95°, respectively. As for the packing mode, to take advantage of the capacious space around the planar picolinamide motif, two **3a** molecules could assemble in the head-to-tail mode. The aryl hydrogens on the B rings could interact with the carbonyl oxygens of the other molecule to form H-bonding (O1 ... H1, 2.85 Å; O1 ... H2, 2.75 Å; O2 ... H3, 2.91 Å). The aforementioned dimers would interlace zigzag to form weak intermolecular π–π interactions. The shortest distances between the aryl D and E rings were around 3.5 Å. These weak intermolecular interactions, like H-bonding and π–π stacking, were able to fix the molecular conformations in the solid-state, thus inhibiting the internal rotations and non-radiative relaxation and inducing the AIE property.

To gain additional insight, density functional theory (DFT) and time-dependent density functional theory calculations (TD-DFT) (Adamo and Jacquemin, 2013) of **3a** were performed with Gaussian09 suite of programs (Frisch et al., 2009). The combination of m062x/6–311 g** was applied in both cases (Zhao and Truhlar, 2008). As shown in **Figure 5**, both the HOMO and LUMO orbitals were delocalized over the picolinamide backbone. However, the electron density distribution of HOMO and LUMO was mainly localized at acyl aniline motif and pyridyl group, respectively. The electron-density contribution of boron in both orbitals were negligible, being 0.80% (HOMO) and 0.48% (LUMO). The HOMO and LUMO orbitals were spatially separated by the boron atom, rendering limited overlap between these two orbitals. Then, TD-DFT calculations on the DFT-optimized structure suggested that lowest energy transition (S0→S1) involves mostly the HOMO and the LUMO orbitals, indicating a possible ligand-to-ligand charge transfer character.

In conclusion, using readily available and stable aryl trifluoroborates as the BAr_2 sources, the picolinamide-based diaryl boronyl complexes have been synthesized for the first time. These propeller-type five-membered complexes exhibit very weak fluorescence in organic solvents and intense fluorescence in their aggregation/solid-state, showing classical AIE properties, which should originate from the confinement of molecular conformations and the inhibited internal rotations when these molecules assemble.

EXPERIMENTAL SECTION

General Information

Unless otherwise noted, all reactions were carried out under an air atmosphere. Analytical thin-layer chromatography (TLC) was performed on glass plates coated with 0.25 mm 230–400 mesh silica gel containing a fluorescent indicator. Visualization was accomplished by exposure to a UV lamp. All the products in this article are compatible with standard silica gel chromatography. Column chromatography was performed on silica gel (200–300 mesh). Eluent generally contained ethyl acetate (EA), petroleum ether (PE) and triethylamine (TEA).

NMR spectra were measured on a Bruker Ascend 400 spectrometer and chemical shifts (δ) are reported in parts per million (ppm). ^{1}H NMR spectra were recorded at 400 MHz in NMR solvents and referenced internally to corresponding solvent resonance, and ^{13}C NMR spectra were recorded at 101 MHz and referenced to corresponding solvent resonance. Coupling constants are reported in Hz with multiplicities denoted as s (singlet), d (doublet), t (triplet), q (quartet), m (multiplet) and br (broad). Infrared spectra were collected on a Thermo Fisher Nicolet 6700 FT-IR spectrometer using ATR (Attenuated Total Reflectance) method. Absorption maxima (ν max) are reported in wavenumbers (cm^{-1}). High resolution mass spectra (HRMS) were acquired on Thermo Scientific LTQ Orbitrap XL with an ESI source. Melting points were measured with a micro-melting point apparatus.

Commercial reagents, including picolinoyl chloride hydrochloride, aniline, naphthalen-1-amine, Mn, *p*-toluenesulfonyl chloride, Na_2CO_3 and All potassium trifluoroborate, were purchased from commercial sources and used as received unless otherwise stated.

Preparation of 2-Pyridinecarboxamide

*N-phenylpicolinamide **(1a)**.* The target product was prepared according to a literature procedure (Li et al., 2014). The product was isolated by flash chromatography as a white solid (1.64 g, 90%): ^{1}H NMR (400 MHz, $CDCl_3$) δ 10.03 (s, 1H), 8.62 (d, *J* = 4.4 Hz, 1H), 8.31 (d, *J* = 7.6 Hz, 1H), 7.96–7.87 (m, 1H), 7.82–7.76 (m, 2H), 7.51–7.45 (m, 1H), 7.43–7.36 (m, 2H), 7.15 (t, *J* = 7.2 Hz, 1H). ^{13}C{^{1}H} NMR (101 MHz, $CDCl_3$) δ 162.0, 149.9, 148.0, 137.8, 137.7, 129.1, 126.5, 124.3, 122.4, 119.7, 77.4, 77.1, 76.7.

N-(naphthalen-1-yl)picolinamide ***(1v)***. The target product was prepared according to a literature procedure.[14] The product was isolated by flash chromatography as a white solid (2.03 g, 89%): ^{1}H NMR (400 MHz, $CDCl_3$) δ 10.77 (s, 1H), 8.75–8.70 (m, 1H), 8.46–8.34 (m, 2H), 8.11 (d, *J* = 8.4 Hz, 1H), 7.98–7.89 (m, 2H), 7.71 (d, *J* = 8.4 Hz, 1H), 7.63–7.50 (m, 4H). ^{13}C{^{1}H} NMR (101 MHz, $CDCl_3$) δ 162.3, 150.1, 148.2, 137.8, 134.1, 132.4, 128.9, 126.6, 126.4, 126.3, 126.3, 126.0, 126.0, 125.9, 125.1, 122.5, 120.8, 120.5, 119.0, 118.6, 109.7, 77.4, 77.1, 76.7.

Typical Experimental Procedures

General Procedure A

A flame-dried 25 ml vial was placed with a magnetic stir bar. Then, *N*-phenylpicolinamide (29.7 mg, 0.15 mmol, 1.0 equiv), potassium trifluoro(phenyl)borate (138.0 mg, 0.75 mmol, 5.0 equiv), Mn (82.0 mg, 0.15 mmol, 1.0 equiv), *p*-toluenesulfonyl chloride (71.5 mg, 0.375 mmol, 2.5 equiv) and Na_2CO_3 (79.5 mg, 0.075 mmol, 0.50 equiv) as a base, and react with acetonitrile as the reaction solvent at 130°C for 24 h. After the completion of the reaction and concentration, the crude product was purified by column chromatography (silica gel) to give the target product, using PE/EtOAc/DCM the eluent.

Preparation and characterization data for isolated products:

Compounds **3a**—**3w** are unknown compounds. $^{1}H/^{13}C$ NMR, melting point, IR, data HRMS (ESI) m/z for these compounds are provided herein.

1,1,2-triphenyl-1,2-dihydro-3H-1λ⁴,8λ⁴-[1,3,2]diazaborolo[1,5-a]pyridin-3-one ***(3a)***. The product was isolated by flash chromatography as a yellow-green solid (53.8 mg, 99%): mp: 186.4–189.4°C; ^{1}H NMR (400 MHz, $CDCl_3$) δ 8.41–8.34 (m, 2H), 8.19 (td, *J* = 8.0, 1.2 Hz, 1H), 7.58 (dd, *J* = 12.4, 6.4 Hz, 1H), 7.55–7.51 (m, 2H), 7.37 (dd, *J* = 7.6, 4.0 Hz, 4H), 7.27–7.20 (m, 6H), 7.16 (t, *J* = 7.9 Hz, 2H), 7.02 (dd, *J* = 1.2, 7.6 Hz, 1H). $^{13}C\{^{1}H\}$ NMR (101 MHz, $CDCl_3$) δ 161.4, 142.4, 141.6, 140.0, 135.8, 133.7, 128.4, 127.9, 127.3, 127.2, 125.0, 124.8, 122.5, 77.5, 77.2, 76.8. HRMS (ESI), m/z calcd for $C_{24}H_{19}BN_2ONa^+$ $(M + Na)^+$ 385.1483, found 385.1485. IR (cm^{-1}): 3,074, 3,009, 1,663, 1,489, 1,348, 762, 702.

1,1-di([1,1′-biphenyl]-4-yl)-2-phenyl-1,2-dihydro-3H-1λ⁴,8λ⁴-[1,3,2]diazaborolo[1,5-a]pyridin-3-one ***(3b)***. The product was isolated by flash chromatography as a yellow-green solid (57.9 mg, 75%): mp: 289.0–290.7°C; ^{1}H NMR (400 MHz, $CDCl_3$) δ 8.46 (dd, *J* = 15.6, 5.6 Hz, 2H), 8.28 (t, *J* = 7.2 Hz, 1H), 7.72–7.68 (m, 1H), 7.65–7.57 (m, 6H), 7.53–7.47 (m, 8H), 7.44–7.39 (m, 4H), 7.34–7.29 (m, 2H), 7.22 (dd, *J* = 7.6, 2.0 Hz, 2H), 7.06 (t, *J* = 7.2 Hz, 1H). $^{13}C\{^{1}H\}$ NMR (101 MHz, $CDCl_3$) δ 161.3, 148.9, 142.4, 141.6, 141.2, 139.9, 139.8, 134.1, 128.7, 128.4, 127.2, 127.1, 127.0, 126.5, 125.0, 124.6, 122.5, 77.4, 77.2, 76.7. HRMS (ESI), m/z calcd for $C_{36}H_{27}BN_2ONa^+$ $(M + Na)^+$ 537.2109, found 537.2111. IR (cm^{-1}): 3,058, 3,015, 1,680, 1,495, 1,348, 740, 686.

1,1-bis(3-bromophenyl)-2-phenyl-1,2-dihydro-3H-1λ⁴,8λ⁴-[1,3,2]diazaborolo[1,5-a]pyridin-3-one ***(3c)*** The product was isolated by flash chromatography as a yellow-green solid (49.9 mg, 64%): mp: 203.5–204.5°C; ^{1}H NMR (400 MHz, $CDCl_3$) δ 8.48–8.40 (m, 1H), 8.38–8.28 (m, 3H), 7.78–7.72 (m, 2H), 7.43–7.35 (m, 6H), 7.25–7.19 (m, 2H), 7.17–7.08 (m, 3H). $^{13}C\{^{1}H\}$ NMR (101 MHz, $CDCl_3$) δ 161.2, 148.6, 143.1, 141.6, 139.0, 135.9, 135.8, 132.0, 130.5, 129.8, 128.6, 127.6, 125.6, 124.9, 122.9, 77.4, 77.1, 76.8. HRMS (ESI), m/z calcd for $C_{24}H_{17}BBr_2N_2ONa^+$ $(M + Na)^+$ 542.9672, found 542.9680. IR (cm^{-1}): 3,058, 1,674, 1,489, 1,348, 762, 692.

2-phenyl-1,1-divinyl-1,2-dihydro-3H-1λ⁴,8λ⁴-[1,3,2]diazaborolo[1,5-a]pyridin-3-one ***(3d)*** The product was isolated by flash chromatography as a yellow-green solid (22.4 mg, 57%): mp: 78.9–80.0°C; ^{1}H NMR (400 MHz, $CDCl_3$) δ 8.40 (d, *J* = 5.6 Hz, 1H), 8.34–8.22 (m, 2H), 7.93–7.85 (m, 2H), 7.75 (t, *J* = 6.0 Hz, 1H), 7.38–7.31 (m, 2H), 7.14 (t, *J* = 7.2 Hz, 1H), 6.30 (dd, *J* = 19.6, 13.2 Hz, 2H), 5.57 (dd, *J* = 13.2, 3.2 Hz, 2H), 5.32 (dd, *J* = 19.6, 3.6 Hz, 2H). $^{13}C\{^{1}H\}$ NMR (101 MHz, $CDCl_3$) δ 160.6, 149.0, 142.1, 141.0, 140.3, 128.4, 126.5, 124.7, 124.6, 123.7, 122.3, 77.4, 77.1, 76.8. HRMS (ESI), m/z calcd for $C_{16}H_{15}BN_2ONa^+$ $(M + Na)^+$ 285.1170, found 285.1173. IR (cm^{-1}): 3,047, 2,928, 1,668, 1,495, 1,360, 757, 686.

1,1-bis(3-fluorophenyl)-2-phenyl-1,2-dihydro-3H-1λ⁴,8λ⁴-[1,3,2]diazaborolo[1,5-a]pyridin-3-one ***(3e)*** The product was isolated by flash chromatography as a yellow-green solid (34.6 mg, 58%): mp: 152.3–154.6°C; ^{1}H NMR (400 MHz, $CDCl_3$) δ 8.43 (d, *J* = 8.0 Hz, 1H), 8.37–8.27 (m, 2H), 7.72 (t, *J* = 6.4 Hz, 1H), 7.44 (d, *J* = 7.6 Hz, 2H), 7.25–7.16 (m, 4H), 7.13–7.04 (m, 3H), 7.00 (dd, *J* = 10.4, 1.2 Hz, 2H), 6.92 (td, *J* = 8.4, 2.0 Hz, 2H). $^{13}C\{^{1}H\}$ NMR (101 MHz, $CDCl_3$) δ 164.0, 161.6, 161.2, 148.8, 143.0, 141.5, 139.3, 129.6, 129.5, 128.9, 128.9, 128.5, 127.4, 125.4, 124.8, 122.8, 119.8, 119.6, 114.3, 114.1, 77.4, 77.1, 76.8. ^{19}F NMR (376 MHz, $CDCl_3$) δ -113.78. HRMS (ESI), m/z calcd for $C_{24}H_{17}BF_2N_2ONa^+$ $(M + Na)^+$ 421.1294, found 421.1297. IR (cm^{-1}): 3,068, 1,680, 1,495, 1,354, 762, 702.

1,1-bis(4-bromophenyl)-2-phenyl-1,2-dihydro-3H-1λ⁴,8λ⁴-[1,3,2]diazaborolo[1,5-a]pyridin-3-one ***(3f)*** The product was isolated by flash chromatography as a yellow-green solid (39.0 mg, 50%): mp: 250.0–251.3°C; ^{1}H NMR (400 MHz, $CDCl_3$) δ 8.42 (d, *J* = 8.0 Hz, 1H), 8.34–8.28 (m, 2H), 7.72 (t, *J* = 6.4 Hz, 1H), 7.47–7.41 (m, 2H), 7.36 (d, *J* = 8.0 Hz, 4H), 7.23–7.16 (m, 6H), 7.07 (t, *J* = 7.6 Hz, 1H). $^{13}C\{^{1}H\}$ NMR (101 MHz, $CDCl_3$) δ 161.1, 148.8, 142.9, 141.4, 139.3, 135.2, 131.0, 128.5, 127.4, 125.4, 124.6, 122.8, 121.9, 77.4, 77.1, 76.7. HRMS (ESI), m/z calcd for $C_{24}H_{17}BBr_2N_2ONa^+$ $(M + Na)^+$ 542.9672, found 542.9680. IR (cm^{-1}): 3,068, 1,674, 1,489, 1,354, 762, 698.

2-phenyl-1,1-di-p-tolyl-1,2-dihydro-3H-1λ⁴,8λ⁴-[1,3,2]diazaborolo[1,5-a]pyridin-3-one ***(3g)*** The product was isolated by flash chromatography as a yellow-green solid (36.9 mg, 63%): mp: 240.9–241.9°C; ^{1}H NMR (400 MHz, $CDCl_3$) δ 8.41–8.35 (m, 2H), 8.24–8.18 m, 1H), 7.64–7.56 (m, 1H), 7.28 (d, *J* = 8.0 Hz, 4H), 7.20–7.14 (m, 2H), 7.07 (d, *J* = 7.6 Hz, 4H), 7.05–7.00 (m, 1H), 2.31 (s, 6H). $^{13}C\{^{1}H\}$ NMR (101 MHz, $CDCl_3$) δ 161.2, 148.8, 142.2, 141.5, 140.1, 136.6, 133.7, 128.6, 128.2, 127.0, 124.8, 124.6, 122.3, 77.4, 77.1, 76.8, 21.3. HRMS (ESI), m/z calcd for $C_{26}H_{23}BN_2ONa^+$ $(M + Na)^+$ 413.1796, found 413.1799. IR (cm^{-1}): 3,020, 1,674, 1,489, 1,348, 768, 686.

1,1-bis(4-chlorophenyl)-2-phenyl-1,2-dihydro-3H-1λ⁴,8λ⁴-[1,3,2]diazaborolo[1,5-a]pyridin-3-one ***(3h)*** The product was isolated by flash chromatography as yellow-green solid (43.3 mg, 67%): mp: 202.0–206.3°C; ^{1}H NMR (400 MHz, DMSO-*d6*) δ 8.74 (d, *J* = 5.6 Hz, 1H), 8.56 (t, *J* = 7.6 Hz, 1H), 8.42 (d, *J* = 7.8 Hz, 1H), 7.99 (t, *J* = 6.4 Hz, 1H), 7.47 (d, *J* = 8.0 Hz, 2H), 7.35–7.25 (m, 8H), 7.19 (t, *J* = 7.6 Hz, 2H), 7.02 (t, *J* = 7.2 Hz, 1H). $^{13}C\{^{1}H\}$ NMR (101 MHz, DMSO-*d6*) δ 161.6, 147.3, 145.0, 142.8, 140.3, 135.5, 132.5, 129.5, 128.7, 128.1, 124.9, 124.1, 123.0, 40.6, 40.4, 40.2, 40.0, 39.8, 39.6, 39.4. HRMS (ESI), m/z calcd for $C_{24}H_{17}BCl_2N_2ONa^+$ $(M + Na)^+$ 453.0703, found 453.0707. IR (cm^{-1}): 3,080, 1,674, 1,489, 1,360, 1,082, 768.

1,1-bis(4-(tert-butyl)phenyl)-2-phenyl-1,2-dihydro-3H-1λ⁴,8λ⁴-[1,3,2]diazaborolo[1,5-a]pyridin-3-one ***(3i)*** The product was isolated by flash chromatography as a yellow-green solid (45.5 mg, 64%): mp: 222.6–223.4°C; ^{1}H NMR (400 MHz, $CDCl_3$) δ 8.42–8.34 (m, 2H), 8.17 (td, *J* = 8.0, 1.2 Hz, 1H), 7.62–7.54 (m, 3H), 7.32 (d, *J* = 8.4 Hz, 4H), 7.28–7.23 (m, 4H), 7.20–7.13 (m, 2H), 7.05–6.97 (m, 1H), 1.29 (s, 18H). $^{13}C\{^{1}H\}$ NMR (101 MHz, $CDCl_3$) δ 161.3, 149.7, 148.7, 142.1, 141.7, 140.2, 133.5, 128.2, 126.9, 124.7, 124.6, 124.6, 122.2, 77.4, 77.1, 76.8, 34.4, 31.4. HRMS (ESI) m/z calcd for $C_{32}H_{35}BN_2ONa^+$ $(M + Na)^+$ 497.2735, found 497.2740. IR (cm^{-1}): 3,080, 2,966, 1,674, 1,489, 1,354, 762, 686.

1,1-bis(benzo[d][1,3]dioxol-5-yl)-2-phenyl-1,2-dihydro-3H-1λ⁴,8λ⁴-[1,3,2]diazaborolo[1,5-a]pyridin-3-one ***(3j)*** The product was isolated by flash chromatography as a yellow-green solid (41.9 mg, 62%): mp: 227.6–229.4°C; ^{1}H NMR (400 MHz, $CDCl_3$) δ 8.37–8.33 (m, 2H), 8.20 (td, *J* = 8.0, 0.8 Hz, 1H), 7.65–7.59 (m, 1H), 7.58–7.52 (m, 2H),

7.23–7.16 (m, 2H), 7.04 (t, *J* = 7.6 Hz, 1H), 6.85 (dd, *J* = 7.6, 1.2 Hz, 2H), 6.79 (d, *J* = 1.2 Hz, 2H), 6.71 (d, *J* = 8.0 Hz, 2H), 5.85 (s, 4H). $^{13}C\{^1H\}$ NMR (101 MHz, $CDCl_3$) δ 161.1, 148.6, 147.3, 146.8, 142.5, 141.5, 139.8, 128.3, 127.1, 125.0, 124.6, 122.4, 113.1, 108.2, 100.4, 77.4, 77.1, 76.8. HRMS (ESI) m/z calcd for $C_{26}H_{19}BN_2O_5Na^+$ $(M + Na)^+$ 473.1279, found 473.1281. IR (cm^{-1}): 3,063, 2,884, 1,680, 1,484, 1,348, 1,234, 1,039, 768.

1,1-bis(4-fluorophenyl)-2-phenyl-1,2-dihydro-3H-1λ⁴,8λ⁴-[1,3,2] diazaborolo[1,5-a]pyridin-3-one ***(3k)*** The product was isolated by flash chromatography as a yellow-green solid (46.6 mg, 78%): mp: 176.1–177.9°C; ^1H NMR (400 MHz, $CDCl_3$) δ 8.40 (d, *J* = 7.6 Hz, 1H), 8.33 (d, *J* = 5.6 Hz, 1H), 8.31–8.24 (m, 1H), 7.71–7.65 (m, 1H), 7.49–7.44 (m, 2H), 7.34–7.27 (m, 4H), 7.22–7.15 (m, 2H), 7.08–7.02 (m, 1H), 6.96–6.90 (m, 4H). $^{13}C\{^1H\}$ NMR (101 MHz, $CDCl_3$) δ 163.8, 161.3, 161.1, 148.7, 142.7, 141.4, 139.7, 135.2, 135.1, 128.7, 128.4, 127.3, 125.2, 124.6, 122.6, 114.9, 114.7, 77.4, 77.1, 76.8. ^{19}F NMR (376 MHz, $CDCl_3$) δ -113.78. HRMS (ESI) m/z calcd for $C_{24}H_{17}BF_2N_2ONa^+$ $(M + Na)^+$ 421.1294, found 421.1298. IR(cm^{-1}): 3,042, 1,680, 1,495, 1,364, 1,164, 774.

1,1-bis(3-(benzyloxy)phenyl)-2-phenyl-1,2-dihydro-3H-1λ⁴,8λ⁴-[1,3,2]diazaborolo[1,5-a]pyridin-3-one ***(3l)*** The product was isolated by flash chromatographyas a yellow-green solid (60.3 mg, 70%): mp: 72.6–74.2°C; ^1H NMR (400 MHz, $CDCl_3$) δ 8.36 (d, *J* = 7.6 Hz, 1H), 8.26 (d, *J* = 5.6 Hz, 1H), 8.20 (td, *J* = 8.0, 1.2 Hz, 1H), 7.59–7.50 (m, 3H), 7.38–7.27 (m, 10H), 7.23–7.15 (m, 4H), 7.07 (t, *J* = 7.2 Hz, 1H), 6.98–6.94 (m, 4H), 6.90–6.84 (m, 2H), 4.97–4.89 (m, 4H). $^{13}C\{^1H\}$ NMR (101 MHz, $CDCl_3$) δ 161.2, 158.3, 148.7, 142.4, 141.6, 139.9, 137.3, 128.9, 128.5, 128.4, 127.8, 127.6, 127.1, 126.3, 125.1, 124.9, 122.4, 120.0, 113.5, 77.4, 77.1, 76.8, 69.8. HRMS (ESI) m/z calcd for $C_{38}H_{31}BN_2O_3Na^+$ $(M + Na)^+$ 597.2320, found 597.2322. IR (cm^{-1}): 3,063, 3,030, 1,680, 1,489, 1,348, 1,229, 762, 692.

1,1-di(naphthalen-2-yl)-2-phenyl-1,2-dihydro-3H-1λ⁴,8λ⁴-[1,3,2] diazaborolo[1,5-a]pyridin-3-one ***(3m)*** The product was isolated by flash chromatography as a yellow-green solid (63.8 mg, 92%): mp: 215.5–217.0°C; ^1H NMR (400 MHz, $CDCl_3$) δ 8.44 (dd, *J* = 4.8, 4.0 Hz, 2H), 8.20 (td, *J* = 7.6, 0.8 Hz, 1H), 7.98–7.95 (m, 2H), 7.83–7.78 (m, 2H), 7.77–7.71 (m, 4H), 7.65–7.61 (m, 2H), 7.60–7.55 (m, 1H), 7.51 (dd, *J* = 8.4, 1.2 Hz, 2H), 7.48–7.40 (m, 4H), 7.19–7.12 (m, 2H), 7.05–6.98 (m, 1H). $^{13}C\{^1H\}$ NMR (101 MHz, $CDCl_3$) δ 161.4, 148.9, 142.5, 141.7, 139.9, 133.5, 133.4, 133.0, 131.0, 128.4, 128.1, 127.6, 127.1,127.1, 125.7, 125.6, 125.1, 124.8, 122.6, 77.4, 77.1, 76.8. HRMS (ESI) m/z calcd for $C_{32}H_{23}BN_2ONa^+$ $(M + Na)^+$ 485.1796, found 485.1797. IR (cm^{-1}): 3,047, 1,668, 1,495, 1,354, 762, 469.

1,1-bis(3-methoxyphenyl)-2-phenyl-1,2-dihydro-3H-1λ⁴,8λ⁴-[1,3,2] diazaborolo[1,5-a]pyridin-3-one ***(3n)*** The product was isolated by flash chromatography as a yellow-green solid (40.5 mg, 64%): mp: 170.9–172.2°C; ^1H NMR (400 MHz, $CDCl_3$) δ 8.378 (t, *J* = 5.2 Hz, 2H), 8.20 (td, *J* = 400, 1.2 Hz, 1H), 7.64–7.58 (m, 1H), 7.55–7.49 (m, 2H), 7.21–7.15 (m, 4H), 7.07–7.01 (m, 1H), 6.96–6.89 (m, 4H), 6.79–6.75 (m, 2H), 3.67 (s, 6H). $^{13}C\{^1H\}$ NMR (101 MHz, $CDCl_3$) δ 161.3, 159.1, 148.7, 142.5, 141.7, 139.9, 128.9, 128.3, 127.1, 125.9, 125.1, 124.9, 122.4, 119.4, 112.2, 77.5, 77.1, 76.8, 55.0. HRMS (ESI) m/z calcd for $C_{26}H_{23}BN_2O_3Na^+$ $(M + Na)^+$ 445.1694, found 445.1699. IR (cm^{-1}): 3,009, 1,668, 1,343, 1,229, 762, 757.

1,1-bis(2-methoxyphenyl)-2-phenyl-1,2-dihydro-3H-1λ⁴,8λ⁴-[1,3,2] diazaborolo[1,5-a]pyridin-3-one ***(3o)*** The product was isolated by flash chromatography as a yellow-green solid (22.2 mg, 35%): mp: 249.1–250.7°C; ^1H NMR (400 MHz, $CDCl_3$) δ 9.13 (d, *J* = 5.6 Hz, 1H), 8.29 (d, *J* = 7.6 Hz, 1H), 8.15 (t, *J* = 6.8 Hz, 1H), 7.62 (d, *J* = 7.6 Hz, 2H), 7.55 (t, *J* = 6.0 Hz, 1H), 7.43–7.39 (m, 2H), 7.23–7.18 (m, 2H), 7.12 (t, *J* = 7.6 Hz, 2H), 6.95 (t, *J* = 7.6 Hz, 1H), 6.84 (t, *J* = 7.2 Hz, 2H), 6.76 (d, *J* = 8.0 Hz, 2H), 3.48 (s, 6H). $^{13}C\{^1H\}$ NMR (101 MHz, $CDCl_3$) δ 162.7, 162.3, 149.6, 142.7, 141.3, 140.9, 137.2, 128.6, 127.9, 125.9, 124.1, 124.0, 121.3, 120.3, 110.4, 77.4, 77.1, 76.8, 54.8. HRMS (ESI) m/z calcd for $C_{26}H_{23}BN_2O_3Na^+$ $(M + Na)^+$ 445.1694, found 445.1695. IR (cm^{-1}): 3,058, 2,933, 1,674, 1,495, 1,360, 1,234, 757.

2-phenyl-1,1-bis(4-(trifluoromethyl)phenyl)-1,2-dihydro-3H-1λ⁴,8λ⁴-[1,3,2]diazaborolo[1,5-a]pyridin-3-one ***(3p)*** The product was isolated by flash chromatography as a yellow-green solid (34.4 mg, 46%): mp: 230.3–232.0°C; ^1H NMR (400 MHz, $CDCl_3$) δ 8.47 (d, *J* = 7.6 Hz, 1H), 8.37 (dd, *J* = 7.6, 1.2 Hz, 1H), 8.35–8.31 (m, 1H), 7.79–7.74 (m, 1H), 7.50 (d, *J* = 8.0 Hz, 4H), 7.46–7.40 (m, 6H), 7.24–7.18 (m, 2H), 7.09 (t, *J* = 7.6 Hz, 1H). $^{13}C\{^1H\}$ NMR (101 MHz, $CDCl_3$) δ 161.1, 148.9, 143.2, 141.4, 139.1, 133.6, 129.8, 129.4, 129.1, 128.6, 127.5, 125.7, 125.5, 124.6, 124.6, 123.0, 123.0, 77.4, 77.0, 76.7. ^{19}F NMR (376 MHz, $CDCl_3$) δ -62.58. HRMS (ESI) m/z calcd for $C_{26}H_{17}BF_6N_2ONa^+$ $(M + Na)^+$ 521.1230, found 521.1236. IR (cm^{-1}): 3,074, 3,036, 1,691, 1,327, 1,109, 762.

1,1-bis(4-(methylthio)phenyl)-2-phenyl-1,2-dihydro-3H-1λ⁴,8λ⁴-[1,3,2]diazaborolo[1,5-a]pyridin-3-one ***(3q)*** The product was isolated by flash chromatography as a yellow-green solid (44.3 mg, 65%): mp: 242.1–243.6°C; ^1H NMR (400 MHz, $CDCl_3$) δ 8.37–8.29 (m, 2H), 8.21 (td, *J* = 7.6, 0.8 Hz, 1H), 7.64–7.57 (m, 1H), 7.53–7.47 (m, 2H), 7.26–7.22 (m, 4H), 7.18–7.12 (m, 2H), 7.11–7.08 (m, 4H), 7.04–6.98 (m, 1H), 2.40 (s, 6H). $^{13}C\{^1H\}$ NMR (101 MHz, $CDCl_3$) δ 161.2, 148.7, 142.5, 141.4, 139.8, 137.2, 134.1, 128.4, 127.1, 125.9, 125.0, 124.5, 122.5, 77.4, 77.1, 76.8, 15.5. HRMS (ESI) m/z calcd for $C_{26}H_{23}BN_2OS_2Na^+$ $(M + Na)^+$ 477.1237, found 477.1238. IR (cm^{-1}): 3,063, 2,916, 1,674, 1,495, 1,375, 1,088, 762.

1,1-bis(2-fluorophenyl)-2-phenyl-1,2-dihydro-3H-1λ⁴,8λ⁴-[1,3,2] diazaborolo[1,5-a]pyridin-3-one ***(3r)*** The product was isolated by flash chromatography as a yellow-green solid (29.3 mg, 49%): mp: 222.9–224.0°C; ^1H NMR (400 MHz, $CDCl_3$) δ 8.85 (d, *J* = 6.0 Hz, 1H), 8.36 (d, *J* = 7.6 Hz, 1H), 8.25 (td, *J* = 8.0, 1.2 Hz, 1H), 7.10–766 (m, 1H), 7.65–7.60 (m, 2H), 7.48–7.42 (m, 2H), 7.25–7.20 (m, 2H), 7.20–7.15 (m, 2H), 7.06–7.01 (m, 3H), 6.92–6.86 (m, 2H). $^{13}C\{^1H\}$ NMR (101 MHz, $CDCl_3$) δ 167.3, 164.9, 161.6, 149.0, 142.5, 142.0, 140.0, 136.9, 136.8, 129.8, 129.7, 128.3, 127.2, 124.6, 123.9, 123.8, 123.8, 122.4, 115.2, 115.0, 77.4, 77.1, 76.7. ^{19}F NMR (376 MHz, $CDCl_3$) δ -103.33. HRMS (ESI) m/z calcd for $C_{24}H_{17}BF_2N_2ONa^+$ $(M + Na)^+$ 421.1294, found 421.1298. IR (cm^{-1}): 3,068, 1,668, 1,495, 1,354, 762, 746.

1,1-bis(3-(tert-butyl)phenyl)-2-phenyl-1,2-dihydro-3H-1λ⁴,8λ⁴-[1,3,2]diazaborolo[1,5-a]pyridin-3-one **(3s)** The product was isolated by flash chromatography as a yellow-green solid (55.5 mg, 78%): mp: 78.1–79.8°C; ^1H NMR (400 MHz, $CDCl_3$) δ 8.45–8.37 (m, 2H), 8.21 (td, *J* = 7.6, 0.8 Hz, 1H), 7.66–7.55 (m, 3H), 7.51–7.45 (m, 2H), 7.32–7.27 (m, 2H), 7.23–7.14 (m, 4H), 7.08–7.01 (m, 3H), 1.25 (s, 18H). $^{13}C\{^1H\}$ NMR (101 MHz, $CDCl_3$) δ 161.3, 149.9, 148.9, 142.3, 141.7, 140.0, 131.6, 130.2,

128.2, 127.4, 127.0, 125.1, 125.0, 123.9, 122.4, 77.5, 77.1, 76.8, 34.7, 31.5. HRMS (ESI) m/z calcd for $C_{32}H_{35}BN_2ONa^+$ $(M + Na)^+$ 497.2735, found 497.2740. IR (cm^{-1}): 2,966, 1,680, 1,489, 1,354, 757, 713.

2,2′-(3-oxo-2-phenyl-2,3-dihydro-1H-1λ⁴,8λ⁴-[1,3,2]diazaborolo [1,5-a]pyridine-1,1-diyl)dibenzonitrile ***(3t)*** The product was isolated by flash chromatography as a yellow-green solid (33.4 mg, 54%): mp: 252.9–253.7°C; ^1H NMR (400 MHz, $CDCl_3$) δ 8.44–8.40 (m, 1H), 8.34–8.29 (m, 2H), 7.75–7.69 (m, 1H), 7.47–7.42 (m, 2H), 7.39–7.34 (m, 4H), 7.22–7.16 (m, 6H), 7.10–7.04 (m, 1H). $^{13}C\{^1H\}$ NMR (101 MHz, $CDCl_3$) δ 161.0, 148.8, 142.9, 141.4, 139.4, 135.2, 131.0, 128.5, 127.3, 125.3, 124.6, 122.8, 121.9, 77.4, 77.1, 76.7. HRMS (ESI) m/z calcd for $C_{26}H_{18}BN_4O+$ $(M + H)^+$ 413.1568, found 413.1563. IR (cm^{-1}): 3,074, 3,025, 1,674, 1,489, 1,348, 762.

1,1-bis(dibenzo[b,d]furan-4-yl)-2-phenyl-1,2-dihydro-3H-1λ⁴,8λ⁴-[1,3,2]diazaborolo[1,5-a]pyridin-3-one ***(3u)*** The product was isolated by flash chromatography as a yellow-green solid (20.3 mg, 25%): mp: 240.3–241.9°C; ^1H NMR (400 MHz, $CDCl_3$) δ 9.12 (d, J = 5.6 Hz, 1H), 8.55 (d, J = 7.6 Hz, 1H), 8.31 (t, J = 7.6 Hz, 1H), 7.98–7.90 (m, 4H), 7.71–7.64 (m, 4H), 7.60–7.54 (m, 1H), 7.39–7.34 (m, 2H), 7.33–7.29 (m, 3H), 7.29–7.27 (m, 1H), 7.24 (d, J = 7.6 Hz, 2H), 7.15 (t, J = 7.9 Hz, 2H), 7.00 (t, J = 7.2 Hz, 1H).$^{13}C\{^1H\}$ NMR (101 MHz, $CDCl_3$) δ 162.0, 159.6, 155.5, 149.8, 142.6, 142.3, 140.3, 134.7, 128.2, 126.8, 126.5, 124.6, 124.5, 124.3, 123.2, 122.6, 122.4, 122.1, 120.4, 120.2, 111.3, 77.4, 77.1, 76.7. HRMS (ESI) m/z calcd for $C_{36}H_{23}BN_2O_3Na^+$ $(M + Na)^+$ 565.1694, found 565.1697. IR (cm^{-1}): 3,053, 1,685, 1,446, 1,348, 1,175, 762.

2-(naphthalen-1-yl)-1,1-diphenyl-1,2-dihydro-3H-1λ⁴,8λ⁴-[1,3,2] diazaborolo[1,5-a]pyridin-3-one ***(3v)*** The product was isolated by flash chromatography as a yellow-green solid (49.5 mg, 80%): mp: 251.2–252.5°C; ^1H NMR (400 MHz, $CDCl_3$) δ 8.48 (d, J = 8.0 Hz, 1H), 8.38 (d, J = 5.6 Hz, 1H), 8.30 (t, J = 7.2 Hz, 1H), 7.75–7.67 (m, 3H), 7.58–7.32 (m, 3H), 7.32–7.27 (m, 3H), 7.23–7.15 (m, 3H), 7.14–6.78 (m, 6H). $^{13}C\{^1H\}$ NMR (101 MHz, $CDCl_3$) δ 161.4, 148.9, 142.6, 142.5, 136.0, 134.2, 129.7, 128.0, 127.3, 127.1, 125.4, 125.3, 125.2, 124.2, 124.1, 122.8, 77.4, 77.1, 76.7. HRMS (ESI) m/z calcd for $C_{28}H_{21}BN_2ONa^+$ $(M + Na)^+$ 435.1639, found 435.1636. IR (cm^{-1}): 3,047, 1,674, 1,398, 1,354, 774, 702.

1,1-bis(4-(benzyloxy)phenyl)-2-phenyl-1,2-dihydro-3H-1λ⁴,8λ⁴-[1,3,2]diazaborolo[1,5-a]pyridin-3-one ***(3w)*** The product was isolated by flash chromatography as a yellow-green solid (60.3 mg, 70%): mp: 83.7–85.6°C; ^1H NMR (400 MHz, $CDCl_3$) δ 8.37 (d, J = 7.2 Hz, 2H), 8.22 (t, J = 8.0 Hz, 1H), 7.66–7.54 (m, 3H), 7.44–7.35 (m, 8H), 7.35–7.28 (m, 6H), 7.19 (t, J = 7.6 Hz, 2H), 7.05 (t, J = 7.6 Hz, 1H), 6.89 (d, J = 8.4 Hz, 4H), 5.02 (s, 4H). $^{13}C\{^1H\}$ NMR (101 MHz, $CDCl_3$) δ 161.2, 158.2, 148.8, 142.2, 141.5, 140.1, 137.3, 134.9, 128.6, 128.3, 127.9, 127.6, 127.0, 124.8, 124.6, 122.3, 114.2, 77.4, 77.2, 76.8, 69.8. HRMS (ESI) m/z calcd for $C_{38}H_{31}BN_2O_3Na^+$ $(M + Na)^+$ 597.2320, found 597.2322. IR (cm^{-1}): 3,020, 1,674, 1,592, 1,170, 698.

DATA AVAILABILITY STATEMENT

The original contributions presented in the study are included in the article/**Supplementary Material**, further inquiries can be directed to the corresponding authors. Additional ^1H and ^{13}C spectra and spectral data for all compounds are available free of charge at http://pubs.acs.org.

AUTHOR CONTRIBUTIONS

GY performed the experiments. LX and YW wrote the manuscript.

ACKNOWLEDGMENTS

We thank the financial support by the National Natural Science Foundation of China (No. 21963010), Shihezi University (CXRC201601 and CXRC201602).

SUPPLEMENTARY MATERIAL

The Supplementary Material for this article can be found online at: https://www.frontiersin.org/articles/10.3389/fchem.2022.856832/full#supplementary-material

REFERENCES

Adamo, C., and Jacquemin, D. (2013). The Calculations of Excited-State Properties with Time-Dependent Density Functional Theory. *Chem. Soc. Rev.* 42, 845–856. doi:10.1039/C2CS35394F

Chen, P.-Z., Niu, L.-Y., Chen, Y.-Z., and Yang, Q.-Z. (2017). Difluoroboron β-diketonate Dyes: Spectroscopic Properties and Applications. *Coord. Chem. Rev.* 350, 196–216. doi:10.1016/j.ccr.2017.06.026

Dou, C., Liu, J., and Wang, L. (2017). Conjugated Polymers Containing B←N Unit as Electron Acceptors for All-Polymer Solar Cells. *Sci. China Chem.* 60, 450–459. doi:10.1007/s11426-016-0503-x

Frisch, M. J., Trucks, G. W., Schlegel, H. B., Scuseria, G. E., Robb, M. A., Cheeseman, J. R., et al. (2009). *Gaussian 09, Revision A*. Wallingford, CT: Gaussian, Inc..

Gong, S., Liu, Q., Wang, X., Xia, B., Liu, Z., and He, W. (2015). AIE-active Organoboron Complexes with Highly Efficient Solid-State Luminescence and Their Application as Gas Sensitive Materials. *Dalton Trans.* 44, 14063–14070. doi:10.1039/C5DT01525A

Huang, Z., Wang, S., Dewhurst, R. D., Ignat'ev, N. V., Finze, M., and Braunschweig, H. (2020). Boron: Its Role in Energy-Related Processes and Applications. *Angew. Chem. Int. Ed.* 59, 8800–8816. doi:10.1002/anie.201911108

Ito, S., Gon, M., Tanaka, K., and Chujo, Y. (2021). Molecular Design and Application of Luminescent Materials Composed of Group 13 Elements with an Aggregation-Induced Emission Property. *Natl. Sci. Rev.* 8, nwab049. doi:10.1093/nsr/nwab049

Kubota, Y., Tanaka, S., Funabiki, K., and Matsui, M. (2012). Synthesis and Fluorescence Properties of Thiazole-Boron Complexes Bearing a β-Ketoiminate Ligand. *Org. Lett.* 14, 4682–4685. doi:10.1021/ol302179r

Li, Q., Zhang, S.-Y., He, G., Ai, Z., Nack, W. A., and Chen, G. (2014). Copper-Catalyzed Carboxamide-Directed Ortho Amination of Anilines with Alkylamines at Room Temperature. *Org. Lett.* 16, 1764–1767. doi:10.1021/ol500464x

Liu, Z., Jiang, Z., Yan, M., and Wang, X. (2019). Recent Progress of BODIPY Dyes With Aggregation-Induced Emission. *Front. Chem.* 7, 712. doi:10.3389/fchem.2019.00712

Luo, J., Xie, Z., Lam, J. W. Y., Cheng, L., Tang, B. Z., Chen, H., et al. (2001). Aggregation-induced Emission of 1-Methyl-1,2,3,4,5-Pentaphenylsilole. *Chem. Commun.*, 1740–1741. doi:10.1039/B105159H

Mei, J., Leung, N. L. C., Kwok, R. T. K., Lam, J. W. Y., and Tang, B. Z. (2015). Aggregation-Induced Emission: Together We Shine, United We Soar!. *Chem. Rev.* 115, 11718–11940. doi:10.1021/acs.chemrev.5b00263

Mellerup, S. K., and Wang, S. (2019). Boron-based Stimuli Responsive Materials. *Chem. Soc. Rev.* 48, 3537–3549. doi:10.1039/C9CS00153K

Min, X., Yi, F., Han, X.-L., Li, M., Gao, Q., Liang, X., et al. (2022). Targeted Photodynamic Therapy Using a Water-Soluble Aggregation-Induced Emission Photosensitizer Activated by an Acidic Tumor Microenvironment. *Chem. Eng. J.* 432, 134327. doi:10.1016/j.cej.2021.134327

Nitti, A., Botta, C., Forni, A., Cariati, E., Lucenti, E., and Pasini, D. (2020). Crystallization-induced Room-Temperature Phosphorescence in Fumaramides. *CrystEngComm* 22, 7782–7785. doi:10.1039/D0CE01253J

Qi, Y., Cao, X., Zou, Y., and Yang, C. (2021). Color-tunable Tetracoordinated Organoboron Complexes Exhibiting Aggregation-Induced Emission for the Efficient Turn-On Detection of Fluoride Ions. *Mater. Chem. Front.* 5, 2353–2360. doi:10.1039/D1QM00046B

Sawazaki, T., Shimizu, Y., Oisaki, K., Sohma, Y., and Kanai, M. (2018). Convergent and Functional-Group-Tolerant Synthesis of B-Organo BODIPYs. *Org. Lett.* 20, 7767–7770. doi:10.1021/acs.orglett.8b03138

Shiu, Y.-J., Cheng, Y.-C., Tsai, W.-L., Wu, C.-C., Chao, C.-T., Lu, C.-W., et al. (2016). Pyridyl Pyrrolide Boron Complexes: The Facile Generation of Thermally Activated Delayed Fluorescence and Preparation of Organic Light-Emitting Diodes. *Angew. Chem. Int. Ed.* 55, 3017–3021. doi:10.1002/anie.201509231

Virgili, T., Forni, A., Cariati, E., Pasini, D., and Botta, C. (2013). Direct Evidence of Torsional Motion in an Aggregation-Induced Emissive Chromophore. *J. Phys. Chem. C* 117, 27161–27166. doi:10.1021/jp4104504

Wang, X., Wu, Y., Liu, Q., Li, Z., Yan, H., Ji, C., et al. (2015). Aggregation-induced Emission (AIE) of Pyridyl-Enamido-Based Organoboron Luminophores. *Chem. Commun.* 51, 784–787. doi:10.1039/C4CC07451C

Wang, Z., Cheng, C., Kang, Z., Miao, W., Liu, Q., Wang, H., et al. (2019). Organotrifluoroborate Salts as Complexation Reagents for Synthesizing BODIPY Dyes Containing Both Fluoride and an Organo Substituent at the Boron Center. *J. Org. Chem.* 84, 2732–2740. doi:10.1021/acs.joc.8b03145

Wu, Y., Li, Z., Liu, Q., Wang, X., Yan, H., Gong, S., et al. (2015). High Solid-State Luminescence in Propeller-Shaped AIE-Active Pyridine-Ketoiminate-boron Complexes. *Org. Biomol. Chem.* 13, 5775–5782. doi:10.1039/C5OB00607D

Yan, N., Wang, F., Wei, J., Song, J., Yan, L., Luo, J., et al. (2019). Highly Emissive B←N Unit Containing Four-Coordinate C,N-Chelated Organoboron Compound for the Detection of Fluoride Ions. *Dyes Pigm.* 166, 410–415. doi:10.1016/j.dyepig.2019.03.057

Yan, W., Hong, C., Long, G., Yang, Y., Liu, Z., Bian, Z., et al. (2014). Synthesis, crystal Structures and Photophysical Properties of Novel boron-containing Derivatives of Phenalene with Bright Solid-State Luminescence. *Dyes Pigm.* 106, 197–204. doi:10.1016/j.dyepig.2014.03.017

Yang, K., Zhang, G., and Song, Q. (2018). Four-coordinate Triarylborane Synthesis via cascade B-Cl/C-B Cross-Metathesis and C-H Bond Borylation. *Chem. Sci.* 9, 7666–7672. doi:10.1039/C8SC02281J

Yang, T., Tang, N., Wan, Q., Yin, S.-F., and Qiu, R. (2021). Recent Progress on Synthesis of N,N′-Chelate Organoboron Derivatives. *Molecules* 26, 1401. doi:10.3390/molecules26051401

Yin, Y., Chen, Z., Li, R.-H., Yuan, C., Shao, T.-Y., Wang, K., et al. (2021). Ligand-Triggered Platinum(II) Metallacycle with Mechanochromic and Vapochromic Responses. *Inorg. Chem.* 60, 9387–9393. doi:10.1021/acs.inorgchem.1c00233

Zhao, Y., and Truhlar, D. G. (2008). The M06 Suite of Density Functionals for Main Group Thermochemistry, Thermochemical Kinetics, Noncovalent Interactions, Excited States, and Transition Elements: Two New Functionals and Systematic Testing of Four M06-Class Functionals and 12 Other Functionals. *Theor. Chem. Account.* 120, 215–241. doi:10.1007/s00214-007-0310-x

Zu, W., Day, C., Wei, L., Jia, X., and Xu, L. (2020). Dual Aminoquinolate Diarylboron and Nickel Catalysed Metallaphotoredox Platform for Carbon-Oxygen Bond Construction. *Chem. Commun.* 56, 8273–8276. doi:10.1039/D0CC03230A

Conflict of Interest: The authors declare that the research was conducted in the absence of any commercial or financial relationships that could be construed as a potential conflict of interest.

Publisher's Note: All claims expressed in this article are solely those of the authors and do not necessarily represent those of their affiliated organizations, or those of the publisher, the editors and the reviewers. Any product that may be evaluated in this article, or claim that may be made by its manufacturer, is not guaranteed or endorsed by the publisher.